Paper
Int'l J. of Aeronautical & Space Sci. 17(1), 54–63 (2016)
DOI: http://dx.doi.org/10.5139/IJASS.2016.17.1.54

IJASS
International Journal of Aeronautical and Space Sciences

Fault Tolerant Control of Hexacopter for Actuator Faults using Time Delay Control Method

Jangho Lee* and Hyoung Sik Choi**

Flight Control Team, Korea Aerospace Research Institute, Daejeon 34133, Republic of Korea

Hyunchul Shim***

Department of Aerospace Engineering, Korea Advanced Institute of Science and Technology, Daejeon 34141, Republic of Korea

Abstract

A novel attitude tacking control method using Time Delay Control (TDC) scheme is developed to provide robust controllability of a rigid hexacopter in case of single or multiple rotor faults. When the TDC scheme is developed, the rotor faults such as the abrupt and/or incipient rotor faults are considered as model uncertainties. The kinematics, modeling of rigid dynamics of hexacopter, and design of stability and controllability augmentation system (SCAS) are addressed rigorously in this paper. In order to compare the developed control scheme to a conventional control method, a nonlinear numerical simulation has been performed and the attitude tracking performance has been compared between the two methods considering the single and multiple rotor faults cases. The developed control scheme shows superior stability and robust controllability of a hexacopter that is subjected to one or multiple rotor faults and external disturbance, i.e., wind shear, gust, and turbulence.

Key words: Hexacopter, Actuator Fault, Fault Tolerant Control, Time Delay Control, Attitude Hold

1. Introduction

Over the past decades, a keen interest on aerial robot has been growing indefinitely. In fact, aerospace industries have focused on aerial robot in lieu of manned aircraft for difficult and dangerous flight missions. Especially, a demand of multi-rotor has been increased drastically and it has been widely adopted in many applications such as broadcasting images, forest fire monitoring, indoor navigation, and so on. Since it has capability of vertical take-off and landing (VTOL), hovering, and easy to flight, the application of a multi-rotor is almost unlimited. Most recently, a multi-rotor is used even for a pizza delivery [22]. In order to perform wide variety of missions successfully, for example surveillance, taking images at the dangerous environments, etc., capability of hovering at the specific location will be a key requirement of a multi-rotor. Furthermore, as an inner loop of a guidance and navigation control loop, attitude hold controller is essential for a hovering maneuver. However, there is no way to stabilize attitudes and to maintain controlled flight of a quadrotor with a conventional control schemes when any one of the motors experiences a fault. Actually, multi-rotor aircraft has not actuators but rotors. The attached rotors on the multi-rotor have a function as other aircraft's actuator through varying the rotor speed. As an effort to resolve the issues, several important researches have been conducted to design a fault tolerant control law for a multi-rotor aircraft. However, there are still remaining issues need to be resolved. Several researches have been performed in the area of fault tolerant control law design of the multi-rotor aircraft with the multi motor faults but few control schemes are available [1, 2]. Y. M. Zhang et al. presented active fault tolerant control scheme for actuator failures based on a two-state adaptive Kalman filter [3]. A similar problem was considered for thrust distribution of an underwater unmanned vehicle using the control allocation scheme [4].

* Senior Researcher: jh7677@kari.re.kr
** Ph. D: chs@kari.re.kr
*** Professor, Corresponding author: hcshim@kaist.ac.kr

Received: February 6, 2015 Revised: November 15, 2015 Accepted: : January 14, 2016

http://ijass.org pISSN: 2093-274x eISSN: 2093-2480

The gain scheduled PID control technique was employed to compensate actuator fault due to overall loss in power of all motors in quadrotor UAV [1]. Although, fault tolerant controller (FTC) for a single actuator failure has been developed, FTC was never successfully implemented for multiple faults of a multi-rotor UAV. In order to apply FTC for multiple faults successfully, system stability and fault tolerance of the controller are major topics need to be addressed. A harsh flight environment, i.e., atmospheric turbulence, wind gust, or limited space in indoor building structure, increases likelihood of malfunction of motors. One or multiple motor failures might be directly resulted of losing UAV and consequently safety issues can be arisen as a major concern if it crashes at the residential area or heavily populated city area.

In order to deal with this issue properly, two approaches were proposed to develop fault tolerant design capability. One approach is simply increasing the number of rotors. This idea is adopted in this paper so that a hexacopter instead of a quadrotor is used as a test bed. The other is introducing a variety of actuation devices. One of the excellent methods of the latter approach is proposed by P. Sequi-Gasco et al. [2]. In their research, proposed new dual actuator tilting concept demonstrates a fault tolerable capability even with two actuator faults. And performance of the proposed reconfigurable concept was verified using the control allocation scheme. However, the dual actuator tilting was not able to successfully maintain its attitudes, especially altitude, when any one of the actuators failure occurs. This might be a major drawback of a quadrotor even the novel actuator titling concept is applied. The proposed method also shows several limitations to apply for the quadrotor with a motor fault situation. One of them is that the quadrotor system will become more complicated in both mechanically and electrically in order to implement the proposed dual axis tilting system. Unfortunately, the complicated system with many additional parts may have high chances to increase the failure rate, i.e., mean time between accidents (MTBA). And in their research, only two types of faults, single actuator fault and pair of adverse motors were considered.

In order to deal with component failures appropriately, the aerospace industries have been widely adopting FTC. R. J. Patton provides excellent overview of FTC [5]. Generally, FTC can be classified into two types, passive and active FTC. The controller with the passive FTC is designed to be robust enough to encompass as many as possible faults. This approach does not require fault detection and diagnosis schemes or controller reconfiguration. Extensive studies on passive FTC have been performed to develop the attitude controller for multi-rotor vehicle considering actuator faults [1, 2, 6]. The passive FTC has an advantage that can be implemented as a fixed controller. It can tolerate, however, only limited predetermined faults and may not be able to properly response to faults that are out of design scope. Moreover, sacrificing nominal performance is inevitable to achieve robustness to certain faults.

On the other hand, the active FTC which is used in this paper with a time delay control method can response adaptively to fault events with the blessing of a reconfiguration mechanism that allows to maintain stability and acceptable performance of the system. Since the active FTC shows promising advantages to overcome preceding drawbacks of the passive FTC, it has drawn interests from many researchers to design aerial vehicle attitude control [7]. A dynamic neural network scheme was presented8 to detect and isolate the fault of aircraft. Detecting actuator faults in a tetrahedron configuration was investigated [9]. An iterative learning observer-based fault detection and diagnosis mechanism was developed [10] to estimate time-varying thrust faults. Also, genetic algorithm such as neural network and adaptive neural network schemes were proposed to cope with the faults of aircraft control surfaces using the reconfigurable flight controller [11, 12]. Although various fault tolerant control schemes are available to perform attitude hold maneuver, most of these available schemes have two drawbacks: first the desired attitude is not able to maintain when there are multiple motor faults, and secondly the attitude tracking problem is solved without considering external disturbance, i.e., wind shear, gust, and so on. These two important factors need to be appropriately considered so that the multi-rotor vehicle is able to maintain controllability and safety at normal conditions as well as motor fault conditions.

In this paper, a reliable control scheme for the attitude tracking control is presented and a hexacopter vehicle is selected as a test bed platform. The developed control scheme successfully maintains control authority with two fault conditions considered: abruptly disabled motor torque and continuously decreased motor torque. Especially, the developed technique is able to achieve stable attitude tacking maneuver with a wind gust situation along with rotor fault conditions. Once faults occurs in multi-rotor UAV, yaw attitude is hard to be controlled. Therefore the attitude hold means the pitch and roll attitude when fault occurs except yaw axis in this paper. The developed approach is shown in Fig. 1. The developed scheme demonstrates reliable and accurate attitude hold control authority that is robust enough to overcome external disturbances and also stable enough to cope with the severe actuator fault conditions. The effective control system is accomplished by designing a TDC

SCAS module.

The following sections are devoted to describe mathematical modeling of the rigid hexacopter UAV dynamics, actuator faults modeling, and derivation of fault tolerant control scheme with multiple rotor faults. In order to verify the developed control scheme, nonlinear numerical simulation is performed for a hexacopter UAV that are implemented in the Matlab/Simulink® environment. Conclusions and future works are addressed in Section 5.

2. Mathematical Model and Problem Formulation

The following notation is used throughout this paper. The vector $[x\ y\ z]^T$ and $[v_x\ v_y\ v_z]^T$ describe position and velocity of the hexacopter in the inertia frame, respectively. And angular rate and Euler angles in body frame are represented as $[p\ q\ r]^T$ and $[\phi\ \theta\ \psi]^T$, respectively.

2.1 Dynamic Model of Hexacopter

In order to describe a hexacopter dynamic, let us consider an inertial frame I and body fixed frame B, as shown in the Figure 2 where the X-Y plane represents the ground surface. The positive Z-axis of the inertial frame is defined as upward from the ground. The origin of the body frame is assumed to be at the center of gravity of the hexacopter. The transformation from the body frame to the inertial frame can be formulated by three successive axis rotations, Z→Y→X sequences, as shown in Figure 2. The yaw angle (ψ) is rotated w.r.t the Z-axis first. This is followed by the pitch angle (θ) rotation w.r.t. the Y-axis, and finally, the roll angle (ϕ) is rotated w.r.t. the new X-axis. This coordinate transformation can be summarized as the directional cosine matrix defined in Eq. (1) [13].

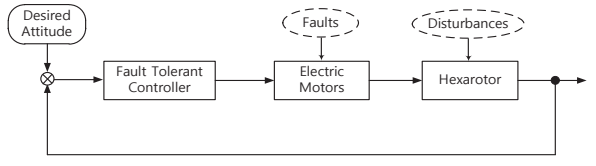

Fig. 1. Structure of Fault-Tolerant Controller

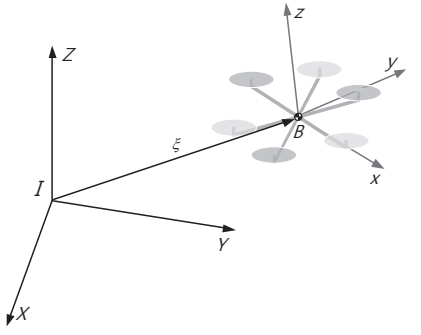

Fig. 2. Position and Orientation of Hexacopter

The positive Z-axis of the inertial frame is defined as upward from the ground. The origin of the body frame is assumed to be at the center of gravity of the hexacopter. Three successive rotations, $Z\rightarrow Y\rightarrow X$ transformation is performed to convert the Euler angle in the body fixed frame to the inertia frame as shown in Fig. 2. In order to convert the Euler angles from body fixed frame to inertial frame, the yaw angle (ψ) is rotated w.r.t the Z-axis first. This is followed by the pitch angle (θ) rotation w.r.t. the Y-axis, and finally, the roll angle (ϕ) is rotated w.r.t. the new X-axis. This coordinate transformation can be summarized as the directional cosine matrix defined in Eq. (1) [13].

$$C^{B/I}(\phi,\theta,\psi) = C_X(\phi)C_Y(\theta)C_Z(\psi) = \begin{bmatrix} c\theta c\psi & c\theta s\psi & -s\theta \\ -c\phi s\psi + s\phi s\theta c\psi & c\phi c\psi + s\phi s\theta s\psi & s\phi c\theta \\ s\phi s\psi + c\phi s\theta c\psi & -s\phi c\psi + c\phi s\theta s\psi & c\phi c\theta \end{bmatrix} \quad (1)$$

where s and c are shorthand forms for sine and cosine respectively.

The equations of motion of a rigid body that is subjected to the sum of forces and torques at the center of mass can be expressed as Newton-Euler equation [14, 15]. The equations in the body fixed frame are shown in Eq. (2).

$$\begin{bmatrix} \mathbf{F} \\ \boldsymbol{\tau} \end{bmatrix} = \begin{bmatrix} m\mathbf{I}_{3\times3} & \mathbf{0} \\ \mathbf{0} & \mathbf{I} \end{bmatrix} \begin{bmatrix} \dot{\mathbf{V}} \\ \dot{\boldsymbol{\omega}} \end{bmatrix} + \begin{bmatrix} \boldsymbol{\omega} \times m\mathbf{V} \\ \boldsymbol{\omega} \times \mathbf{I}\boldsymbol{\omega} \end{bmatrix} \quad (2)$$

where F and τ denote the force and torque vector respectively. m is the mass, $\mathbf{I} \in \mathrm{R}^{3x3}$ is the inertia matrix, V is the linear velocity vector, and ω denotes the body angular velocity vector.

Figure 3 shows the hexacopter frame system. The rigid body equations of motion in the body fixed frame are formulated [16, 17] as

$$\begin{cases} \dot{\boldsymbol{\xi}} = \mathbf{v} \\ \dot{\mathbf{v}} = -g\hat{k} + C_{\hat{k}}^{I/B}\left(\dfrac{b}{m}\sum_{i=1}^{6}\Omega_i^2\right) \\ \dot{C}^{I/B} = C^{I/B}\omega_{\times} \\ \mathbf{I}\dot{\boldsymbol{\omega}} = -\boldsymbol{\omega} \times \mathbf{I}\boldsymbol{\omega} - \sum_{i=1}^{6} J_r(\boldsymbol{\omega}\times\hat{k})\Omega_i + \boldsymbol{\tau} \end{cases} \quad (3)$$

The notation $\xi=[x\ y\ z]^T$ denote the position vector of the hexacopter frame center and v denote the linear velocity expressed in the inertial frame. g and $\hat{k}$ denote the acceleration of gravity and the z axis respectively and

J_r denotes rotor inertia. $\omega_\times$ denotes the skew-symmetric matrix, such that $\omega_\times v=\omega\times v$ indicates the vector cross product $\times$ with any vector $v\in R^3$. The vector F_B in the body fixed frame represents the principal non-conservative forces applied to the hexacopter airframe due to the aerodynamic forces of the rotors [16]. Eq. (3) is approximated that the airframe drag is negligible.

The thrust applied to the hexacopter airframe is defined as Eq. (4).

$$T=\sum_{i=1}^{6}|f_i|=b\left(\sum_{i=1}^{6}\Omega_i^2\right) \tag{4}$$

where f_i denotes the lift generated by an i-th rotor, b denotes the thrust factor which is always $b>0$, and Ω denotes the rotor speed. The parameter b is a linear approximation to a constantly varying property which is proportional to various conditions, for example, air density, number of blades, and hexacopter geometry, and so on.

The aerodynamic torque inputs applied to the hexacopter structure are shown in Eq. (5) though Eq. (7). The Eqs. (5), (6), and (7) represent the positive pitch moment, rolling moment, and yawing moment, respectively. The torque is consisted of aerodynamic lift and drag generated by the rotors.

$$\tau_\phi=lb\sin(\pi/3)(\Omega_2^2+\Omega_3^2-\Omega_5^2-\Omega_6^2) \tag{5}$$

$$\tau_\theta=lb(-\Omega_1^2+\Omega_4^2)+lb\cos(\pi/3)(-\Omega_2^2+\Omega_3^2+\Omega_5^2-\Omega_6^2) \tag{6}$$

$$\tau_\psi=d(\Omega_1^2-\Omega_2^2+\Omega_3^2-\Omega_4^2+\Omega_5^2-\Omega_6^2) \tag{7}$$

where l represents the displacement of the rotors with respect to the center of mass of the hexacopter and d denotes the drag factor. Finally, based on the above equations, the full model of the hexacopter can be rewritten as Eq. (8) [17].

$$\begin{cases}
\ddot{x}=\dfrac{(\sin\phi\sin\psi+\cos\phi\sin\theta\cos\psi)}{m}T\\
\ddot{y}=\dfrac{(-\sin\phi\cos\psi+\cos\phi\sin\theta\sin\psi)}{m}T\\
\ddot{z}=-g+\dfrac{\cos\phi\cos\theta}{m}T\\
\dot{p}=qr\left(\dfrac{I_y-I_z}{I_x}\right)+\dfrac{1}{I_x}\tau_\phi-\dfrac{J_r}{I_x}q\Omega_G\\
\dot{q}=pr\left(\dfrac{I_z-I_x}{I_y}\right)+\dfrac{1}{I_y}\tau_\theta-\dfrac{J_r}{I_y}p\Omega_G\\
\dot{r}=pq\left(\dfrac{I_x-I_y}{I_z}\right)+\dfrac{1}{I_z}\tau_\psi
\end{cases} \tag{8}$$

where $\Omega_G=\Omega_1-\Omega_2+\Omega_3-\Omega_4+\Omega_5-\Omega_6$.

2.2 Hexacopter Configuration

As shown in Fig. 3, two pairs of rotors are spinning opposite direction, i.e., the rotors (1,3,5) spin counter clockwise and the rotors (2,4,6) spin clockwise view from the top to bottom. In so doing, the reaction torque due to the spinning rotors can be cancelled out each other. The lifting force generated by a rotor is simply proportional to the angular speed of the rotor. Therefore the positive vertical translational motion can be introduced by increasing the six rotor angular speed simultaneously. Increasing the rotor angular speed of (2,3) and decreasing (5,6) will produce positive roll maneuver coupled with the negative lateral translation. Similarly, the positive pitch maneuver can be achieved by increasing rotor angular speed of (3,4,5) and decreasing (1,2,6). And this will be coupled with the positive forward translation. Yaw can be achieved by introducing unbalance torque between the two pairs of counter spinning rotors.

For a hexacopter, the relationship, denoted as Γ, between the rotor angular speed (Ω) and the 4 body-axis accelerations can be described as Eq. (9). Given desired and moments, the required rotor speeds can be solved using the inverse of the constant matrix Γ.

$$\begin{bmatrix}T\\ \tau_\phi\\ \tau_\theta\\ \tau_\psi\end{bmatrix}=\Gamma\begin{bmatrix}\Omega_1^2\\ \Omega_2^2\\ \Omega_3^2\\ \Omega_4^2\\ \Omega_5^2\\ \Omega_6^2\end{bmatrix} \tag{9}$$

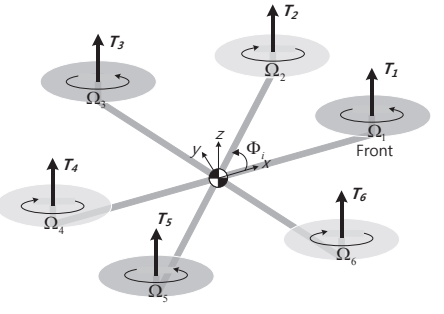

Fig. 3. Notation for Hexacopter Equations of Motion

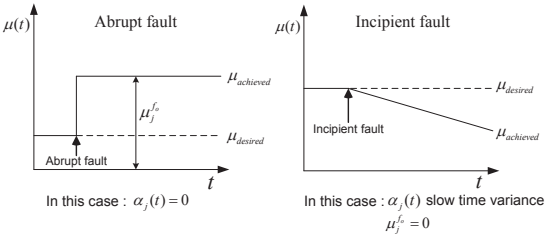

Fig. 4. Typical Types of Actuator Faults

where, Γ denotes maps that effect of each rotor speeds to the vehicle motion to the thrust(T), rolling, pitching and yawing moment domain.

$$\Gamma = \begin{bmatrix} b & b & b & b & b & b \\ 0 & lb\sin\left(\frac{\pi}{3}\right) & lb\sin\left(\frac{\pi}{3}\right) & 0 & -lb\sin\left(\frac{\pi}{3}\right) & -lb\sin\left(\frac{\pi}{3}\right) \\ -lb & -lb\cos\left(\frac{\pi}{3}\right) & lb\cos\left(\frac{\pi}{3}\right) & lb & lb\cos\left(\frac{\pi}{3}\right) & -lb\cos\left(\frac{\pi}{3}\right) \\ d & -d & d & -d & d & -d \end{bmatrix}$$

2.3 Actuator Fault Modeling

The actuator is the key element of the hexacopter that generates necessary forces to control the airframe. The actuator of the hexacopter is a controllable small electric motor attached at the end of the six shaft frame structure. Typically four possible faults are conceivable, such as zero torque, i.e., disabled motor (F1), decreased torque (F2), offset torque (F3), and spinning opposite direction as opposed to what it designed for (F4). Even though the hexacopter has redundant actuators, occurrence of F3 or F4 fault of one of the six motors could lead loss of control authority without any means of recovery. Therefore, these types of catastrophic fault conditions are excluded from the scope of current research and only the F1 and F2 faults are mainly considered in this paper. The multiple-redundant system along with the fault tolerant control design, especially for air vehicle, is so important to increase safety and reliability of system. Many research efforts have been devoted to fault tolerant control design considering actuator faults in the past decades. Figure 4 shows two typical types of actuator faults of aircraft system, i.e., abrupt fault and incipient fault. The abrupt fault means a "hard" type failure and disturbs the control system significantly in a brief space of time. The abrupt fault may be caused by many sources, electric short circuits, actuator stuck fault, damages of control surfaces due to foreign object debris (FOB), or impact to hard objects, just to name a few. Due to the nature of sudden change of its phase, the incidence of this type of fault can be easily detected. On the other hand, the incipient fault is progressively developed and affects control system for a long time. This type of fault is considered as a "soft" type fault. Since this type of fault grows slowly, it is challenging to identify the incidence [18].

F1 and F2 types of failure for each actuator can be modeled as single and/or multiple faults in the time domain.

$$\mu_j^f = \alpha_j(t)\mu_j^n + \mu_j^{f_o}, \quad \forall j \in 1, 2, \ldots \tag{10}$$

where μ_j^n represents the nominal torque for the j-th motor, $\mu_j^{f_o}$ is the constant offset torque representing a constant speed spinning of the respective motors, and $\alpha_j(t)$ denotes a gain degradation factor represented by a scalar value between 0 and 1. The nominal torque condition can be obtained with $\alpha_j(t)$=1, and $\mu_j^{f_o}$=0 in Eq. (10) and yields $\mu_j^f = \mu_j^n$. Setting both $\alpha_j(t)$ and $\mu_j^{f_o}$ to zero introduces the F1 type failure for the j-th motor which leads to μ_j^f=0 from Eq. (10). Similarly, setting $\alpha_j(t)$ value between 0 and 1, $\mu_j^{f_o}$ to zero of Eq. (10) leads to the F2 type failure for the j-th motor and the resultant torque is expressed as $\mu_j^f = \alpha\mu_j^n$. Also, setting $\alpha_j(t)$=1 and $\mu_j^{f_o}$<0 leads to the F3 type failure.

The preceding motor fault numerical models are simulated in Fig. 5. A sine function is used as a reference input to the motor. The actual motor torques are computed with and without faults. Two parameters are considered. One is the fault evolution rate (a) and the other is the gain degradation factor (α). The scalar $a_j > 0$ denotes the unknown fault evolution rate. A small value of aj characterizes slowly developing fault, also known as an incipient fault. For a large value of a_j, the time profile approaches to a step function that represents an abrupt fault. Having those two parameters, two types of faults, the motor stop (F1) and degraded motor torque (F2) are plotted against with the nominal torque case as shown in Fig. 5.

The motor torque drops to zero with α = 0 and reduces to 50% of the nominal input with α = 0.5. A larger fault evolution rate (a) corresponds to the rapid approach to the final fault torque. The single fault modeling can be expanded to the multiple faults model as described in Eq. (11).

$$\begin{aligned} \mathbf{B}\mathbf{u}^f &= \mathbf{B}\left\{ \begin{pmatrix} \alpha_1(t) & 0 & \cdots & 0 \\ 0 & \alpha_2(t) & \ddots & 0 \\ \vdots & \ddots & \ddots & \vdots \\ 0 & 0 & \cdots & \alpha_6(t) \end{pmatrix} u + \begin{pmatrix} \mu_1^{f_o} \\ \mu_2^{f_o} \\ \vdots \\ \mu_6^{f_o} \end{pmatrix} \right\} \\ &= \mathbf{B}^f\mathbf{u} + \mathbf{B}\boldsymbol{\mu}^{f_o} \end{aligned} \tag{11}$$

Note that **B** is control effectiveness matrix which is represents the relation between the rotor speeds and the

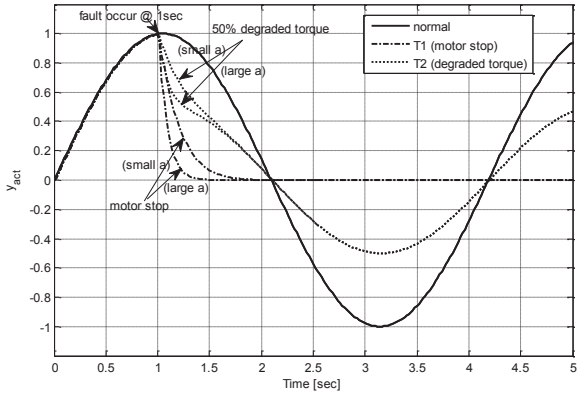

Fig. 5. Actual Motor Fault (F1 : disabled, F2 : degraded motor torque).

vehicle dynamics and also inverse of the Γ in Eq. (9) and $\mathbf{B}^f$ represents the actuator fault distribution matrix related to the normal constant control input matrix **B**.

2.4 Problem Statement

Having the hexacopter rigid body dynamic model, Eq. (8), and the multiple actuator faults model, Eq. (11), a fault tolerant control scheme needs to be designed. The control scheme should be able to stabilize the system as well as track the desired reference command. It should be applicable for both the nominal rotor situation and single or multiple motor faults situation.

3. Fault Tolerant Control Design

3.1 Fault Tolerant Control Scheme with TDC

The TDC control scheme has been studied in many years and well established [19, 21]. Therefore, detailed derivation of the scheme is not covered in this paper, but major concept is reviewed.

A general nonlinear dynamic equation is given as below equation.

$$\dot{\mathbf{x}} = \mathbf{f}(\mathbf{x}, \mathbf{t}) + \mathbf{B}(\mathbf{x}, \mathbf{t})\mathbf{u} + \mathbf{d}(\mathbf{t}) \tag{12}$$

The desired performance of the reference model is presented as Eq. (13)

$$\dot{\mathbf{x}}_\mathbf{d} = \mathbf{A}_\mathbf{d}\mathbf{x}_\mathbf{d} + \mathbf{B}_\mathbf{d}\mathbf{r} \tag{13}$$

where x_d denotes the desired trajectory.

By substituting Eq. (11) into Eq. (12), the nonlinear dynamic equation yields as

$$\dot{\mathbf{x}} = \mathbf{f}(\mathbf{x}, \mathbf{t}) + \mathbf{B}^f(\mathbf{x}, \mathbf{t})\mathbf{u} + \mathbf{B}(\mathbf{x}, \mathbf{t})\boldsymbol{\mu}^{f_o} + \mathbf{d}(\mathbf{t}) \tag{14}$$

where d(t) denotes disturbance.

Introducing estimated control effectiveness matrix($\hat{B}$), Eq. (14) can be rewritten as Eq. (15).

$$\dot{\mathbf{x}} = \hat{\mathbf{f}}(\mathbf{x}, \mathbf{t}) + \hat{\mathbf{B}}\mathbf{u} \tag{15}$$

where $\hat{B}$ denotes estimated control effectiveness which is a constant matrix (or scalar) and represents the known range of B(x,t). From Eqs. (14) and (15), $\hat{\mathbf{f}}(\mathbf{x}, \mathbf{t})$ can be obtained as

$$\hat{\mathbf{f}}(\mathbf{x}, \mathbf{t}) = \mathbf{f}(\mathbf{x}, \mathbf{t}) + [\mathbf{B}^f(\mathbf{x}, \mathbf{t})\mathbf{u} + \mathbf{B}(\mathbf{x}, \mathbf{t})\boldsymbol{\mu}^{f_o} - \hat{\mathbf{B}}\mathbf{u}] + \mathbf{d}(\mathbf{t}) \tag{16}$$

Equation (16) contains all the nonlinear uncertainties and disturbance terms. Using Eqs. (13) and (15), the error dynamics can be expressed as

$$\begin{aligned}\dot{\mathbf{e}} &= \dot{\mathbf{x}}_\mathbf{d} - \dot{\mathbf{x}} = \dot{\mathbf{x}}_\mathbf{d} - \hat{\mathbf{f}}(\mathbf{x}, \mathbf{t}) - \hat{\mathbf{B}}\mathbf{u} \\ &= \mathbf{A}_\mathbf{d}\mathbf{e} + \left[-\hat{\mathbf{f}}(\mathbf{x}, \mathbf{t}) + \mathbf{A}_\mathbf{d}\mathbf{x} + \mathbf{B}_\mathbf{d}\mathbf{r} - \hat{\mathbf{B}}\mathbf{u}\right]\end{aligned} \tag{17}$$

where $e = x_d - x$.

If control input u is defined such that

$$-\hat{\mathbf{f}}(\mathbf{x}, \mathbf{t}) + \mathbf{A}_\mathbf{d}\mathbf{x} + \mathbf{B}_\mathbf{d}\mathbf{r} - \hat{\mathbf{B}}\mathbf{u} = \mathbf{k}\mathbf{e} \tag{18}$$

Rewriting Eq. (18), the computed control input yields as

$$\mathbf{u} = \hat{\mathbf{B}}^{-1}[-\hat{\mathbf{f}}(\mathbf{x}, \mathbf{t}) + \mathbf{A}_\mathbf{d}\mathbf{x} + \mathbf{B}_\mathbf{d}\mathbf{r} - \mathbf{k}\mathbf{e}] \tag{19}$$

Combining Eq. (17) and Eq. (19), the error dynamics can be rearranged as

$$\dot{\mathbf{e}} = (\mathbf{A}_\mathbf{d} + \mathbf{k})\mathbf{e} \tag{20}$$

Assuming the time step L is very small, the time delay estimation can be approximated as

$$\hat{\mathbf{f}}(\mathbf{x}, \mathbf{t}) \cong \hat{\mathbf{f}}(\mathbf{x}, \mathbf{t} - \mathbf{L}) \tag{21}$$

Similarly, Eq. (15) can also be approximated as

$$\hat{\mathbf{f}}(\mathbf{x}, \mathbf{t}) \cong \dot{\mathbf{x}}(\mathbf{t} - \mathbf{L}) - \hat{\mathbf{B}}\mathbf{u}(\mathbf{t} - \mathbf{L}) \tag{22}$$

By substituting Eq. (22) into Eq. (19), $\hat{\mathbf{f}}(\mathbf{x}, \mathbf{t})$ and uncertainty terms are eliminated. The final computed control input is obtained as

$$\mathbf{u} = \mathbf{u}(\mathbf{t} - \mathbf{L}) + \hat{\mathbf{B}}^{-1}[-\dot{\mathbf{x}}(\mathbf{t} - \mathbf{L}) + \mathbf{A}_\mathbf{d}\mathbf{x} + \mathbf{B}_\mathbf{d}\mathbf{r} - \mathbf{k}\mathbf{e}] \tag{23}$$

Eq. (23) is a typical TDC control law. Since internal plant dynamics equation is not included, the TDC control law does not require an exact dynamic model and properties of a rotorcraft. It only requires previous time step quantities, i.e., control input $u(t\text{-}L)$, states $x(t\text{-}L)$ and predefined quantities, i.e., estimated control effectiveness $\hat{B}$ and pre-shaped input matrix B_d.

From Eqs. (17), (18), and (21), the error dynamics can be rearranged as

$$\dot{\mathbf{e}} = \mathbf{A}_\mathbf{d}\mathbf{e} + \left[-\hat{\mathbf{f}}(\mathbf{x}, \mathbf{t}) + \hat{\mathbf{f}}(\mathbf{x}, \mathbf{t} - \mathbf{L}) + \mathbf{k}\mathbf{e}\right] \tag{24}$$

As shown in Eq. (24), the system is stable as long as magnitude of error satisfies the condition specified in Eq. (25).

$$|\mathbf{e}| > \frac{\left|\hat{\mathbf{f}}(\mathbf{x}, \mathbf{t}) - \hat{\mathbf{f}}(\mathbf{x}, \mathbf{t} - \mathbf{L})\right|}{|\mathbf{k} + \mathbf{A}_\mathbf{d}|} \tag{25}$$

where, k is negative quantity and A_d is stable. The Eq. (25) indicates that the error will be bounded only if the system

difference at time t and t-L is small enough. Taking notice of these characteristics of TDC scheme, it is assumed that the hexacopter can have fault tolerant capabilities even in faults occurrence such as system disturbances and unknown parameters of system model.

3.2 SCAS Control Law Design

The conventional PI controller is used to control the heave and yaw channel. In so doing, the much simpler controller is able to implement yet satisfies the purpose of this research. The final TDC control law for the pitch and roll channel can be obtained as Eq. (26) and Eq. (27) [20].

$$u_3 = u_3(t-L) + \hat{m}^{-1}[-\ddot{\theta}(t-L) + \omega_{nd}{}^2(\theta_d - \theta) - 2\zeta_d\omega_{nd}\dot{\theta}] \quad (26)$$

$$u_2 = u_2(t-L) + \hat{l}^{-1}[-\ddot{\phi}(t-L) + \omega_n{}^2(\phi_d - \phi) - 2\zeta\omega_n\dot{\phi}] \quad (27)$$

The pitch and roll attitude hold configuration of TDC are shown in Fig. 6 and Fig. 7 respectively.

4. Numerical Example

A hexacopter numerical model is developed using the dynamics equations, Eqs. (8), in conjunction with the TDC scheme, Eqs. (26) and (27). The developed numerical model is implemented in the Matlab/Simulink® environment to demonstrate the effectiveness and robustness of the developed fault tolerant control scheme. The hexacopter is assumed as a rigid vehicle without being considered flexibility of airframe structure. Two missions, tracking attitudes and holding a desired altitude, are evaluated including F1 and F2 types of actuator faults and external disturbance, i.e., wind shear, gust, and turbulence. Note that the simulation is performed with external disturbance only for the proposed case because the states of hexacopter with PID controller are diverging at the presence of the wind disturbance. These are the most unlikely achievable missions using an ordinary PID controller. The control scheme computes desired output at the current time step using the quantities computed at the previous time step, i.e., the inputs, states, and estimated control effectiveness with pre-shaped input.

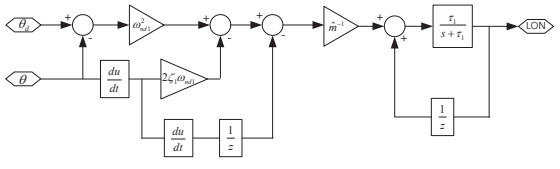

Fig. 6. Pitch Attitude Hold Structure of TDC
($\zeta_{d1} = 0.9,\ \omega_{nd1} = 1.0,\ \hat{m}^{-1} = 5.0,\ \tau_1 = 5.0$)

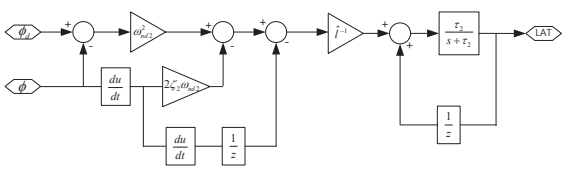

Fig. 7. Roll Attitude Hold Structure of TDC
($\zeta_{d2} = 0.9,\ \omega_{nd2} = 1.5,\ \hat{l}^{-1} = 5.0,\ \tau_2 = 5.0$)

Since the proposed time delay fault tolerant control is developed based on the robustness of the TDC that allows excluding the uncertainty terms as shown in Eq. (23), it is capable of not only stabilizing the system but also performing robust controllability against uncertainties such as model uncertainty and external disturbance.

The full nonlinear 6-DOF rotorcraft dynamics is developed including the equation of motion of a rotorcraft and the actuator dynamic blocks. The actuator bandwidth is 20 rad/s. Without losing accuracy of numerical integration, 0.01 second is selected as the numerical simulation time step, L of Eq. (21). The numerical simulation was conducted considering many parameters, i.e., two types of faults, F1 and F2, three different types of external disturbance, and two control methods, PID and TDC. The F1 fault denotes that the motor #3 is disabled (abrupt fault) at ten second followed by disabled motor #1 (abrupt fault) at twenty second. A half torque of the motor #4 (incipient fault) is introduced at thirty second and is denoted as F2 fault. In order to compare tracking performance, the simulation was conducted using both conventional PID and developed TDC. The pitch and roll attitude hold configuration of PID are shown in Fig. 8 and Fig. 9 respectively.

The simulation starts from zero altitude and reaches target altitude 10 meter. This target altitude should be hold during entire simulation time. Three second later, +5 degree pitch attitude command is injected to the system and then +5 degree roll attitude command is added at five second. As shown in Figs. 10 through 13, both TDC and PID controllers

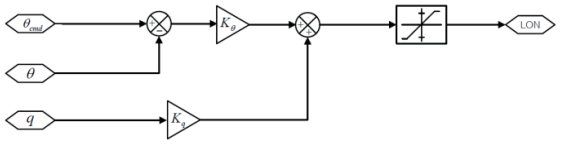

Fig. 8. Pitch Attitude Hold Structure of PID ($K_q = -0.5,\ K_\theta = 0.2$)

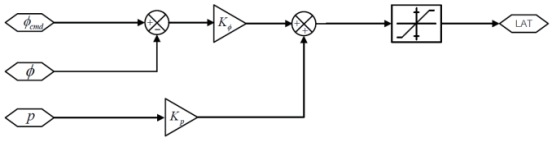

Fig. 9. Roll Attitude Hold Structure of PID ($K_p = 1.0,\ K_\phi = 0.5$)

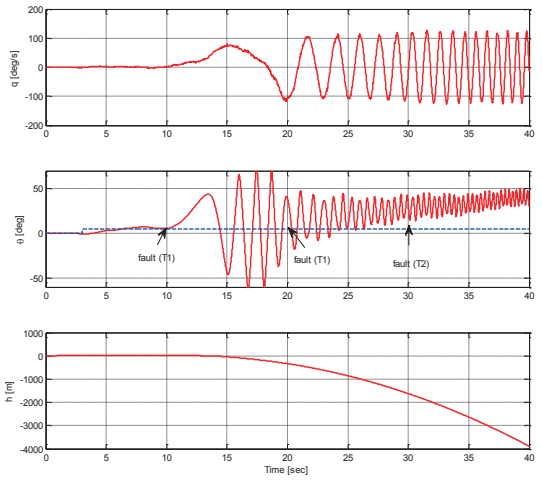

Fig. 10. Time histories of longitudinal states (PID)

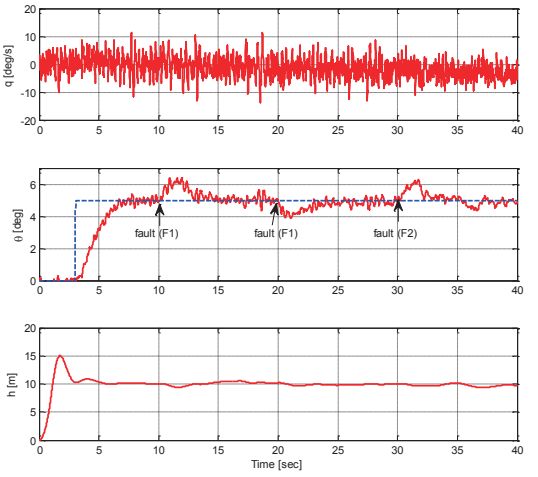

Fig. 12. Time Histories of Longitudinal States (proposed method)

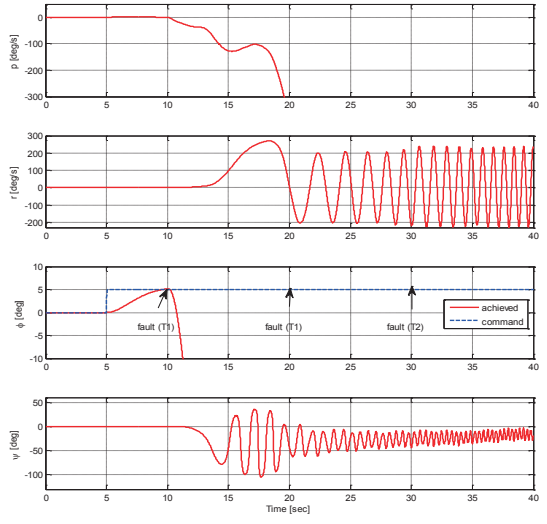

Fig. 11. Time Histories of Lateral States (PID)

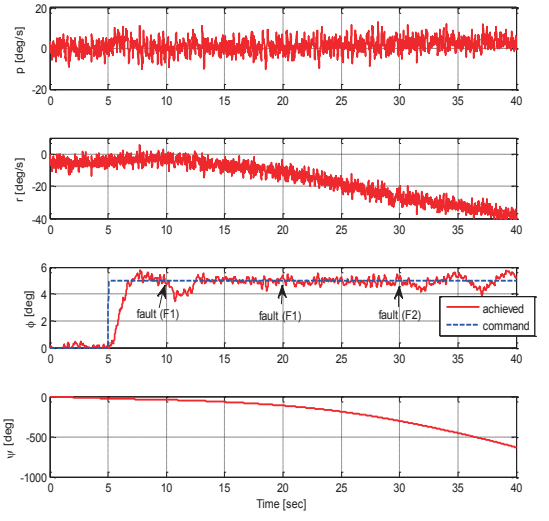

Fig. 13. Time Histories of Lateral States (proposed method)

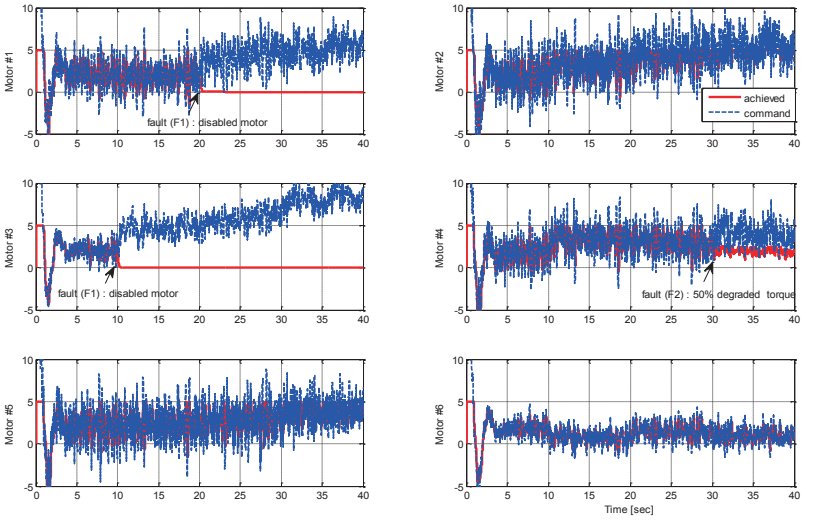

Fig. 14. Control inputs (proposed method)

show similar tracking performance until the faults occur. However, once the F1 fault occurs, the PID controller is not able to track the input command properly. The longitudinal states, q and θ, show oscillating responses with large amplitude. And the PID controller fails to track the pitch attitude (θ) command input. In addition, the altitude drops rapidly from the initial hovering altitude. These results are shown in Fig. 10. Note that the numerical simulation was conducted without bounded altitude despite it drops below zero altitude.

Figure 11 shows time responses of the lateral/directional states with the PID controller. The yaw rate (r) and yaw angle (ψ) show bounded oscillation with very slow convergence to the steady state, but the roll rate (p) and roll angle (ϕ) diverge rapidly right after F1 fault occurs. Apparently these results demonstrate that the conventional PID controller is not able to cope with the motor failure situation at all.

On the other hand, the developed TDC scheme shows promising performance for both nominal and motor failure conditions. The time histories of the longitudinal states with the developed TDC scheme are presented in Fig. 12. When the F1 and F2 faults occur the pitch state (θ) shows small deviation from the input command and tracks back to the command position within 3-4 seconds. Furthermore, the altitude (h) is maintained its targeted altitude regardless of the motor failures indicating robustness of the developed TDC.

Similarly, as shown in Fig. 13, the roll state (ϕ) shows transient maneuver when the F1 and F2 faults are introduced. Briefly after the transient maneuver, however, it traces back the commanded attitudes.

Figure 14 shows the time histories of each motor input that clearly present disabled rotor #1 and #3 and 50% degraded performance of rotor #4. Throughout the entire simulation, external disturbances, i.e., wind shear, gust, and turbulence whose time histories are shown in Fig. 15 are applied to the system. Note that in order to maintain altitude hold mode with the continuous positive pitch and roll attitude command inputs, the yaw angle (ψ) should be allowed to move freely without any bounds.

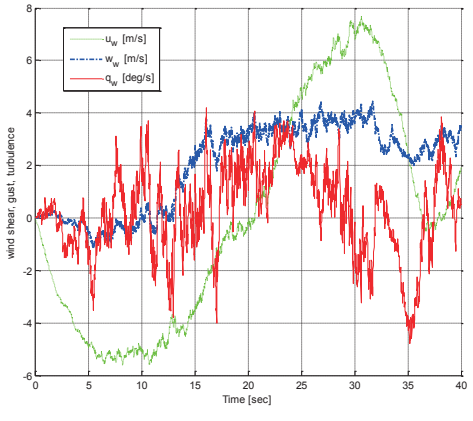

Fig. 15. Wind Shear, Gust, Turbulence

5. Conclusions and Future Works

A fault tolerant control scheme is developed as an attitude tracking system for a hexacopter aircraft. A formulation of fault tolerant control design is developed based on the TDC scheme that allows excluding the internal plant dynamic model and uncertainties. The developed control scheme is effective enough to provide robust control authority for both external disturbances and single or multiple rotor failure situations. The numerical method implemented in the Matlab/Simulink® environment confirms the effectiveness and robustness of the developed fault tolerant control scheme with TDC. The numerical simulation results validate that the proposed TDC is superior in the attitude tracking to PID controller, especially when abrupt and incipient rotor faults are introduced. It requires, however, the accurate inertia information of the hexacopter aircraft. Since only the decreased torque was considered as the incipient rotor fault, the offset torque will be investigated to improve the control reliability in the future. Furthermore, flight tests will be performed to verify the proposed control scheme.

References

[1] Sadeghzadeh, I., Mehta, A., Chamseddine, A. and Zhang, Y., "Active Fault Tolerant Control of a Quadrotor UAV based on Gainscheduled PID Control", *proceedings of the 2012 25th IEEE Canadian Conference on Electrical and Computer Engineering (CCECE)*, Montreal, QC, 2012.

[2] Segui-Gasco, P., Al-Rihani, Y., Shin, H. S. and Savvaris, A., "A Novel Actuation Concept for a Multi Rotor UAV", *Journal of Intelligence & Robotic Systems*, Vol. 74, Issue 1, 2014, pp. 173-191.

[3] Zhang, Y. M. and Jiang, J., "Active fault-tolerant control system against partial actuator failures", *IEE Proceedings of Control Theory Applications*, Vol. 149, No. 1, 2002, pp. 95–104.

[4] Garus. J., "Optimization of Thrust Allocation in the Propulsion System of an Underwater vehicle", *Int. J. Appl. Math. Comput. Sci.*, Vol. 14, No. 4, 2002, pp. 461–467.

[5] Patton, R. J., "Fault Tolerant Control - The 1997 situations(survey)", *IFAC Safe Process '97*, Hull, UK, Vol. 2, 1997, pp. 1033-1055.

[6] Liu, H., "Robust Optimal Attitude Control of

Multirotors", *Proc. of Australasian Conference on Robotics and Automation*, Sydney Australia, 2013.

[7] Xiao, N., Hu, Q., Singhose, W. and Huo, X., "Reaction Wheel Fault Compensation and Disturbance Rejection for Spacecraft Attitude Tracking", *Journal of Guidance, Control, and Dynamics*, Vol. 36, No. 6, 2013, pp. 1565–1575.

[8] Li, Z., Ma, L. and Khorasani, K., "A Dynamic Neural Network-Based Reaction Wheel Fault Diagnosis for Satellites", *International Joint Conference on Neural Networks*, IEEE Publications, Piscataway, NJ, 2006, pp. 3714-3721.

[9] Jiang, T. and Khorasani, K., "A Fault Detection, Isolation and Reconstruction Strategy for a Satellite's Attitude Control Subsystem with Redundant Reaction Wheels", *IEEE International Conference on Systems, Man and Cybernetics, IEEE Publications*, Piscataway, NJ, 2007, pp. 1644–1650.

[10] Chen, B. L. and Nagarajaiah, S., "Linear-Matrix-Inequality-Based Robust Fault Detection and Isolation Using The Eigenstructure Assignment Method", *Journal of Guidance, Control, and Dynamics*, Vol. 30, No. 6, 2007, pp. 1831–1835.

[11] Shin, D. and Kim, Y., "Nonlinear Discrete-Time Reconfigurable Flight Control Systems Using Neural Networks", *IEEE Transactions on Control Systems Technology*, Vol. 14, No. 3, 2006, pp. 408-422.

[12] Shin, D. and Kim, Y., "Reconfigurable Flight Control System Design Using Adaptive Neural Networks", *IEEE Transactions on Control Systems Technology*, Vol. 12, No. 1, 2004, pp. 87-100.

[13] Kim, P., *Rigid Body Dynamics for Beginners,* Charleston, SC, 2013.

[14] Sastry, S., *A mathematical introduction to robotic manipulation*, Boca Raton. FL, 1994.

[15] Chriette, A., "Contribution a la commande et a la modelisation des helicopters, Asservissement visual et commande adaptive", Phd Thesis, 2001.

[16] Hamel, T., Mahony, R., Lozano, R. and Ostrowski, J., "Dynamic modelling and configuration stabilization for an X4-flyer", *Proc. Int. Federation of Automatic Control Symp. (IFAC)*, 2002, pp. 6. (Modeling)

[17] Bouabdallah, S., Murrieri, P. and Siegwart, R., "Design and control of an indoor micro quadrotor", *Proc. IEEE Int. Conf. Robotics and Automation (ICRA)*, Vol. 5, 2004, pp. 4393–4398. (Modeling)

[18] Rachinayani, P. K., "Robust Fault-Tolerant Control for Aircraft Systems", Jawaharlal Nehru Technological University, May. 2002.

[19] Choi, H. S., Lee, S., Lee, J., Kim, E. T. and Shim, H., "Aircraft Longitudinal Auto-Landing Guidance Law Using Time Delay Control Scheme", *Transactions of the Japan Society for Aeronautical and Space Sciences*, Vol. 53, No. 181, 2010, pp. 207-214.

[20] Lee, J., Choi, H. S., Lee, S., Kim, E. T. and Shin, D., "Time Delay Fault Tolerant Controller for Actuator Failures during Aircraft Autolanding", *Transactions of the Japan Society for Aeronautical and Space Sciences*, Vol. 55, No. 3, 2012, pp. 175-182.

[21] Youcef-Toumi K. and Ito, O., "A Time Delay Controller for Systems with Unknown Dynamics", *ASME*, Vol. 112, 1990, pp. 133-142.

[22] http://rt.com/news/167936-russia-drones-pizza-delivery